Nuclear Instruments and Methods in Physics Research B 269 (2011) 1578–1581

Contents lists available at ScienceDirect

Nuclear Instruments and Methods in Physics Research B

journal homepage: www.elsevier.com/locate/nimb

Effect of impact angle and projectile size on sputtering efficiency of solid benzene investigated by molecular dynamics simulations

Bartlomiej Czerwinski [a,*], Lukasz Rzeznik [b], Robert Paruch [b], Barbara J. Garrison [c], Zbigniew Postawa [b]

[a] Goszczynski College, pl. Krasińskiego 1, 34-400 Nowy Targ, Poland
[b] Smoluchowski Institute of Physics, Jagiellonian University, ul. Reymonta 4, 30-059 Kraków, Poland
[c] Department of Chemistry, The Pennsylvania State University, University Park, PA 16802, USA

ARTICLE INFO

Article history:
Received 18 July 2010
Received in revised form 8 December 2010
Available online 15 December 2010

Keywords:
Sputtering
SIMS
SNMS
Molecular dynamics computer simulations
Cluster projectiles
Organic materials

ABSTRACT

Molecular dynamics computer simulations have been used to investigate the effect of the cluster size on the sputtering yield dependence on the impact angle. Ar_{366} and Ar_{2953} cluster projectiles with 14.75 keV of incident energy are directed at the surface of a solid benzene crystal described by a coarse-grained representation at angles between 0° and 70°. It is observed that the shape of the angular dependence of sputtering efficiency is strongly affected by the cluster size. For the Ar_{366} cluster, the sputtering yield only slightly increases with the impact angle, has a broad maximum around 40°, and decreases at larger angles. For the Ar_{2953} cluster, the yield strongly increases with the impact angle, has a maximum around 45° followed by a steep decrease at larger angles. For both investigated cluster projectiles the primary energy is deposited so close to the surface so that the sputtering efficiency only weekly benefits from the shift of the deposited energy profile toward the surface which occurs at larger impact angles. In this study, molecular dynamics computer simulations are used to probe the effect of the impact angle on the efficiency of ejection molecules emitted from solid benzene by 14.75 keV Ar_{366} and Ar_{2953} clusters.

1. Model

Detailed description of molecular dynamics computer simulations used to model cluster bombardment can be found elsewhere [3]. Briefly, the motion of the particles is determined by integrating Hamilton's equations of motion. The forces among the particles are described by a blend of pair-wise additive and many-body potential energy functions. In this study, we use the coarse-grained approach to model argon cluster bombardment of benzene solid. This technique has proven to significantly decrease simulation time while giving results similar to the data obtained with a full atomistic model [1]. However, the downside of the coarse-grained representation is the inability to consider broad-based chemical reactions. Therefore, any conclusions about the chemistry of irradiated samples must be drawn with caution. In this work, each coarse-grained benzene molecule is represented by six CH particles with the mass of 13 amu. A Lennard–Jones potential is used to describe the CH–CH particles located in different molecules. The CH–CH interaction inside a single benzene molecule is described by a Morse potential. Details of a coarse-grained method and appropriate values for the Lennard–Jones and Morse potential parameters can be found in Ref. [1]. Finally, the interactions between Ar atoms in the projectile and between Ar atoms and all other particles in the system are described by a Lennard–Jones potential splined with KrC potential to properly describe high-energy collisions [2]. The model approximating the benzene crystal consists of 307,366 coarse-grained molecules arranged in a hemispherically shaped sample. This shape is different from a parallelepiped that is used in most of sputtering simulations. Selection of such a shape allows us to significantly reduce number of atoms in the sample by elimination of atoms located at the edges, which do not play a noticeable role in sputtering calculations. The radius of the sample is approximately 25.8 nm. The micro crystallite is surrounded by zone of rigid molecules and a Langevin heat bath composed of several layers of molecules kept at 0 K, which is used to prevent pressure waves generated by the cluster projectile impact from reflecting off the crystal boundaries back into the crystallite [3]. Total sputtering yields are calculated as the equivalent number of benzene molecules corresponding to the total organic material removed by a single impact. It has been observed that bombardment with large polyatomic projectiles is a mesoscopic event and little fluctuations in sputtering yields are expected [3]. Therefore, the yields for each incidence angle are calculated from the data obtained from three trajectories corresponding to different points of impact.

2. Results and discussion

The angular dependence of the total sputtering yield of organic material ejected during 14.75 keV Ar_{366} and Ar_{2953} cluster

* Corresponding author. Fax: +48 12 633 7086.
E-mail address: bartlomiej.czerwinski@uj.edu.pl (B. Czerwinski).

0168-583X/$ - see front matter © 2011 Elsevier B.V. All rights reserved.
doi:10.1016/j.nimb.2010.12.026

bombardment of solid benzene is shown in Fig. 1. It is evident that the shape of this dependence is quite different for these two projectiles. In the case of Ar_{366} bombardment, the total sputtering yield only slightly increases with the impact angle, has a broad maximum around 40°, and decreases at larger angles. A similar behavior has been observed previously for C_{60} bombardment of an organic material [4,5] and Ar_n clusters bombarding inorganic samples [5,6]. For Ar_{2953} cluster bombardment the yield strongly increases with the impact angle, has a maximum around 45° followed by a steep decrease at larger angles. The shape recorded for Ar_{2953} bombardment resembles the shape of the impact angle dependence reported in numerous studies with atomic projectiles [7]. Such behavior has been attributed to two counterbalancing processes. The first process is associated with the energy deposition profile being shifted closer to the surface with the increase of the impact angle. For keV atomic projectiles a significant portion of the primary kinetic energy is deposited below the volume of efficient sputtering. A shift of a larger portion of this energy into this volume leads to a yield enhancement. However, an increase of the impact angle above a certain critical value leads also to a significant energy backreflection. As a result, less energy is available for sputtering and the sputtering yield decreases [8]. Such scenario is, however, improbable for keV medium and large cluster bombardment. For these projectiles almost all of the primary kinetic energy is deposited in the volume that can efficiently contribute to sputtering [5]. As a result, the yield only slightly benefits from the modification of the deposited energy profile and the resulting distribution should be rather flat over a wide range of angles, which is indeed observed for Ar_{366} projectile. However, such description cannot account for the yield variation observed for Ar_{2953}.

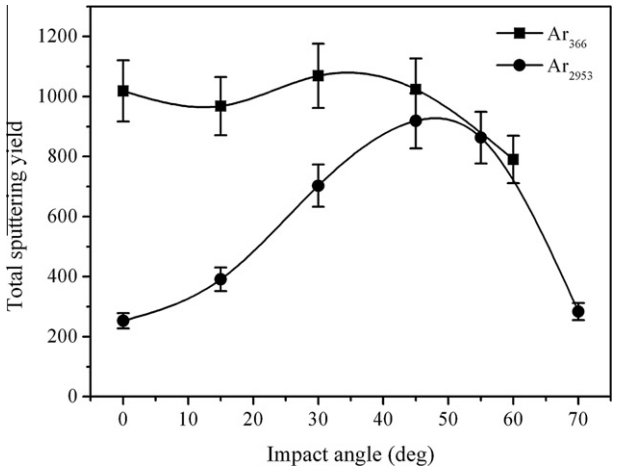

Fig. 1. Total sputtering yield dependence on the impact angle for 14.75 keV Ar_{366} (squares) and Ar_{2953} (circles) projectiles bombardment of solid benzene. The total sputtering yield is expressed as the equivalent number of ejected benzene molecules corresponding to the organic material removal stimulated by a single impact. Solid lines are drawn to guide the eye.

To shed some light on the observed differences, the mechanism of particle ejection stimulated by an impact of Ar_{366} and Ar_{2953} projectiles is delineated. Time snapshots of the motion of particles in the benzene system are shown in Figs. 2 and 3 for Ar_{366} and Ar_{2953}, respectively. The beginning of the arrows depict the position of

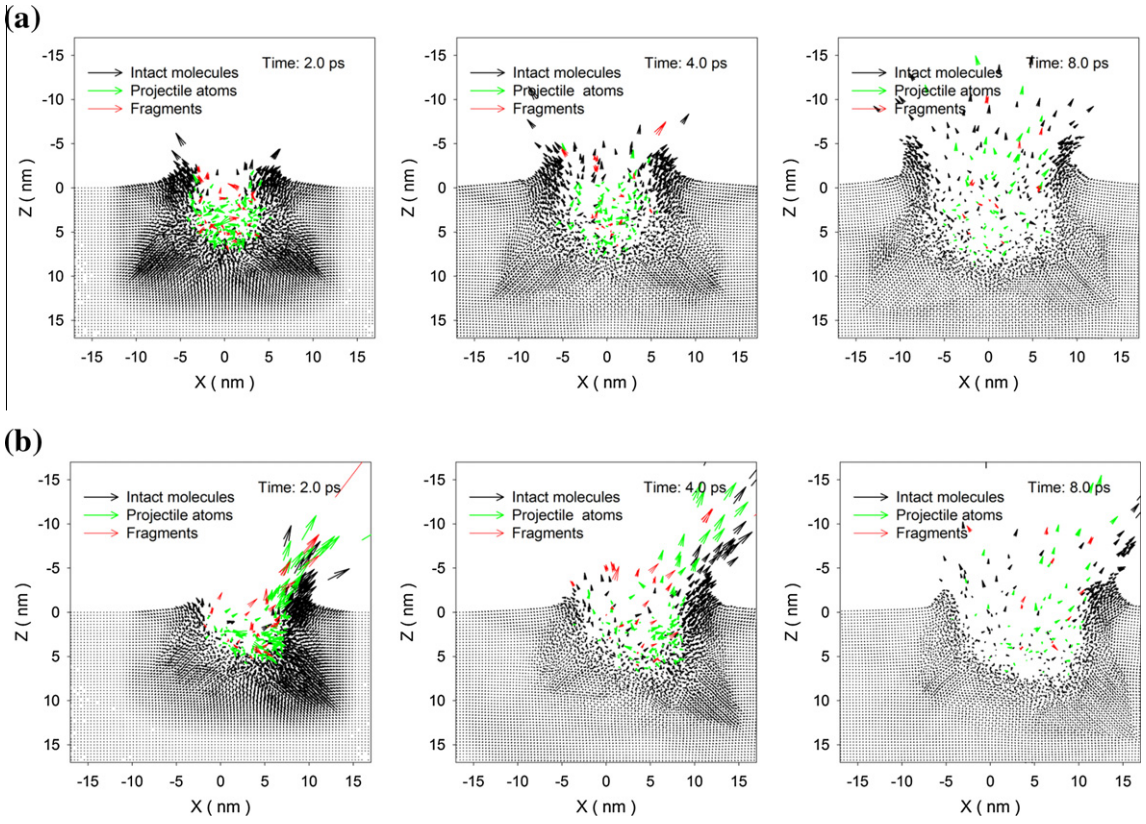

Fig. 2. Time evolution of the ejection events represented by a vector plot illustrating the original position and final position of particles at a given time from the point of impact by 14.75 keV Ar_{366} onto a benzene crystal at 0° (a) and 45° (b) impact angles. Intact molecules are represented by a black vector, fragments by a red/grey vector, while projectile atoms are depicted by a green/thick black vector along the cross sectional view of the crater centered at the impact point. (For interpretation of the references to colour in this figure legend, the reader is referred to the web version of this article.)

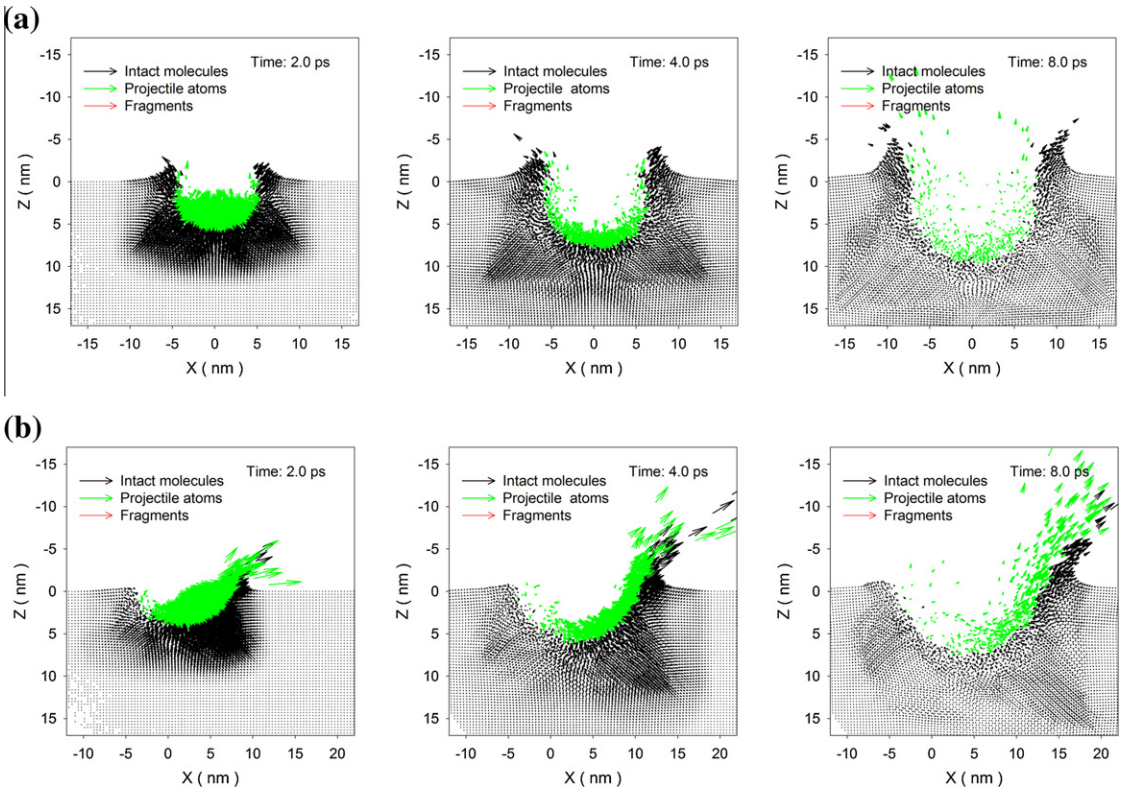

Fig. 3. Time evolution of the ejection events represented by a vector plot illustrating the original position and final position of particles at a given time from the point of impact by 14.75 keV Ar_{2953} onto a benzene crystal at 0° (a) and 45° (b) impact angles. Intact molecules are represented by a black vector, fragments by a red/grey vector, while projectile atoms are depicted by a green/thick black vector along the cross sectional view of the crater centered at the impact point. (For interpretation of the references to colour in this figure legend, the reader is referred to the web version of this article.)

molecules at a given time, while the end of arrows represent positions 0.5 ps later. In this representation, the direction of a given vector represents the direction of the particle motion, while the length of the vector represents its velocity. Fig. 2 presents the time evolution of a thick benzene system bombarded by Ar_{366} cluster projectile at normal (a) and 45° (b) incident angle. The course of events during bombardment is very similar to the one observed for C_{60} [9] and is rather typical for medium-size cluster bombardment. Upon impact, the projectile deposits its kinetic energy at the near surface region. As the projectile travels downward, a localized region of fragmentation is shaped within the film that is nearest to the point of impact. In the early stages of emission, the crater develops and the compression of molecules generates a pressure pulse in a downward direction. This pulse relocates both molecules and fragments laterally in which subsequently energetic molecules are emitted at large polar angles that spatially correspond to areas near the edge of the crater along with fragments as shown in the 2 ps snapshot. The volume of fragmentation obstructs the emission of intact molecules about the surface normal until later times. At later times, however, a significant number of low-energy molecules is ejected predominantly in directions close to the surface normal. At 45° there is a noticeable ejection of high-energy molecules (long arrows) at specular direction along the impact azimuth not present at normal incidence. Nevertheless, still a large number of low-energy molecules is ejected at later-times in directions close to the surface normal. As a consequence, only a small asymmetry is observed in the angular spectrum of ejected molecules as shown in Fig. 4.

When the Ar_{2953} cluster is used for bombardment, processes which lead to ejection of organic material from the surface become somewhat different. The first difference can be observed at normal incidence (Figs. 2a and 3a). Due to a small binding energy between molecules, both argon clusters easily penetrate into the benzene crystal. However, while the spatial integrity of the Ar_{366} cluster is quickly compromised and by 2 ps the projectile atoms are separated and moving at random directions inside the crater or are already ejected. On the other hand, the Ar atoms from Ar_{2953} stay together. They form a layer that effectively blocks particle emission from the bottom of the crater. The benzene molecules are only ejected from the rim of the created crater in the same fluid like motion as observed for Ar_{366}. This blocking effect has already been reported in simulations performed on inorganic materials with large Ar cluster projectiles [10]. This effect combined with particle emission from the sides of a forming crater leads to ejection of atoms and molecules at large polar angles, or so called lateral sputtering [10]. Only after several picoseconds, when the Ar atoms are spread in a larger volume or are already backreflected into the vacuum, then the density of the Ar cloud is reduced to the point where ejection of organic molecules is possible from the bottom of the crater. However, at this time, most of the primary kinetic energy is already carried away from the impact volume. As a result, only a few molecules have sufficient energy to leave the surface and the ejection efficiency is low. This phenomenon combined with a lower energy per atom in the bombarding cluster is responsible for a much lower sputtering yield observed at normal incidence for 14.75 keV Ar_{2953} than Ar_{366} as shown in Fig. 1.

As shown in Fig. 3b, the effectiveness of the blocking mechanism decreases for 45° impact, which leads to increased ejection. However, the effect is not very strong. The most interesting difference in behavior of the system irradiated at 45° as compared to normal bombardment is a formation of an intense flux of Ar atoms "sliding" over the right side of the crater. The interaction of these atoms with weakly bound benzene molecules leads to a significant ejection of organic particles. In this scheme, intact molecules as

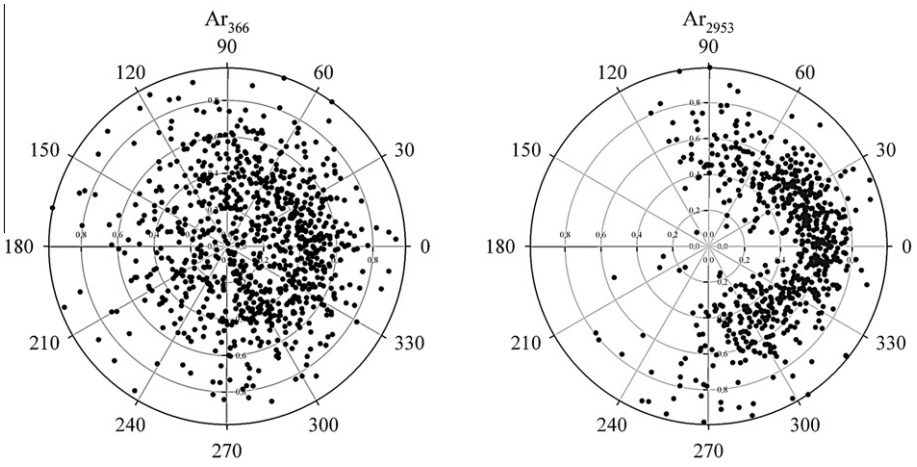

Fig. 4. Polar and azimuthal representation of the ejection directions of intact benzene molecules by 14.75 keV Ar_{366} and 14.75 keV Ar_{2953} projectiles at incidence angle of 45°.

well as organic fragments are "washed out" of the crystal. One consequence of such type of ejection should be a strong azimuthal anisotropy observed in angular emission of benzene molecules. Indeed, as seen in Fig. 4, such anisotropy is pronounced for Ar_{2953} while barely visible for Ar_{366}.

Finally, the shape of the angular dependence of the sputtering yield observed for Ar_{2953} cluster irradiating solid benzene is not universal. Our study performed with the same projectile irradiating silver [4] or the experimental measurements performed on Ag and Cu samples [6] do not exhibit any peculiarities in the shape of the impact angle dependence of Ag and Cu sputtering yields. In fact, the yield variation was very similar to the one presented in Fig. 1 for Ar_{366} cluster. This observation indicates that a difference in sample properties should play a significant role in generating such behavior. There are many differences between Ag and benzene samples. We believe, however, that the most important difference from the point of view of this study is the binding energy of these solids. While the sublimation energy of Ag(111) is 2.3 eV, the sublimation energy of solid benzene is around 0.45 eV [11]. As a result, gentle interactions between "sliding" flux of projectile atoms and the sample particles can be efficient to stimulate ejection from weakly bound solids like benzene, but it may be small for solids in which atoms or molecules are bound by stronger interactions.

3. Conclusions

We have examined the effect of the impact angle and projectile size on the ejection efficiency of particles from solid benzene crystal bombarded by 14.75 keV Ar_{366} and Ar_{2953} clusters. A significant difference in the shape of the total sputtering yield dependence on the impact angle is observed for these two clusters. We attribute this fact to different ejection mechanisms which occur during bombardment by Ar_{366} and Ar_{2953} clusters. In the case of the smaller cluster, the sputtering process is typical for medium-size cluster bombardment. As the projectile travels downward, a localized region of fragmentation is shaped within the film that is nearest to the point of impact. In the early stages of emission, the crater develops and the compression of molecules generates a pressure pulse in a downward direction. This pulse relocates both molecules and fragments laterally in which subsequently energetic molecules are emitted at large polar angles that spatially correspond to areas near the edge of the crater along with fragments. The volume of fragmentation obstructs the emission of intact molecules along the surface normal until later times. At later times, however, a significant number of low-energy molecules is ejected predominantly in directions close to the surface normal. Upon impact, the projectile deposits its kinetic energy at the near surface region the yield only slightly benefits from the modification of the deposited energy profile and the resulting distribution is flat over a wide range of angles. A strong increase of the sputtering yield with the impact angle observed for Ar_{2953} cluster is attributed to the blocking property of large cluster that occurs at low impact angles and, especially, to a "washing off" of weakly bound benzene molecules by a flux of redirected Ar atoms. It is shown that such mechanism occurs for large cluster projectiles irradiating weakly bound solids.

Acknowledgments

The authors would like to thank the Polish Ministry of Science and Higher Education Programs Nos. PB 4097/H03/2007/33 and PB 1247/B/H03/2010/39 and the Chemistry Division of the National Science Foundation Grant No. CHE-0910564 for their financial support of this research. The authors would also like to thank the Pennsylvania State University High Performance Computing Group for use of their computing resources and technical support.

References

[1] E.J. Smiley, Z. Postawa, I.A. Wojciechowski, N. Winograd, B.J. Garrison, Appl. Surf. Sci. 252 (2006) 6436.
[2] R.A. Aziz, M.J. Slaman, Mol. Phys. 58 (1986) 679.
[3] Z. Postawa, B. Czerwinski, M. Szewczyk, E.J. Smiley, N. Winograd, B.J. Garrison, Anal. Chem. 75 (2003) 4402.
[4] L. Rzeznik, R. Paruch, B.J. Garrison, Z. Postawa, This Proceedings.
[5] K.E. Ryan, E.J. Smiley, N. Winograd, B.J. Garrison, Appl. Surf. Sci. 255 (2008) 844.
[6] H. Kitani, N. Toyoda, J. Matsuo, I. Yamada, Nucl. Instrum. Meth. Phys. Res. B 121 (1997) 489.
[7] D.A. Thompson, S.S. Johar, Radiat. Eff. 55 (1981) 91.
[8] W. Eckstein, in: R. Behrisch, W. Eckstein (Eds.), Sputtering by Particle Bombardment III, Springer-Verlag, Berlin Heidelberg, 2007, p. 33.
[9] B. Czerwinski, L. Rzeznik, R. Paruch, B.J. Garrison, Z. Postawa, Vacuum 83 (2009) S95.
[10] Z. Insepov, I. Yamada, Nucl. Instrum. Meth. Phys. Res. B 99 (1995) 248.
[11] E.G. Cox, D.W.J. Cruickshank, J.A.S. Smith, Proc. R. Soc. A 279 (1964) 98.